Articles

Chinese Science Bulletin

Geophysics

April 2010 Vol.55 No.11: 1053−1058
doi: 10.1007/s11434-009-0610-8

Predicting the shock arrival time using 1D-HD solar wind model

ZHANG Ying[1,2*], CHEN JingYi[2] & FENG XueShang[2]

[1] *Institute of Geology and Geophysics, Chinese Academy of Sciences, Beijing 100029, China;*
[2] *State Key Laboratory of Space Weather, Center for Space Sciences and Applied Research, Chinese Academy of Sciences, Beijing 100190, China*

Received April 11, 2009; accepted August 11, 2009

A 1D-HD shock propagation model is established to predict the arrival time of interplanetary shocks at 1 AU. Applying this model to 68 solar events during the period of February 1997 to October 2000, it is found that our model could be practically equivalent to the STOA, ISPM and HAFv.2 models in forecasting the shock arrival time. The absolute error in the transit time from our model is not larger than those of the other three models for the same sample events. Also, the prediction test shows that the relative error of our model is ⩽10% for 31% of all events, ⩽30% for 75%, and ⩽50% for 84%, which is comparable to the relative errors of the other models. These results might demonstrate a potential capability of our model in terms of real-time forecasting.

interplanetary shocks, shock propagation model, arrival time prediction

Citation: Zhang Y, Chen J Y, Feng X S. Predicting the shock arrival time using 1D-HD solar wind model. Chinese Sci Bull, 2010, 55: 1053−1058, doi: 10.1007/s11434-009-0610-8

Solar activities are important drivers of space weather and play important roles in leading to adverse solar-terrestrial environment. It is well known that various kinds of solar transient activities such as solar flares, disappearing filaments, and coronal mass ejections (CMEs) are responsible for strong interplanetary (IP) disturbances and corresponding non-recurrent geomagnetic disturbances. The IP shocks in the solar wind plasma associated with CMEs, solar flares, and stream-stream interactions herald the initiation of geomagnetic storms if sufficiently long and sufficiently large-magnitude southward components of the interplanetary magnetic field exist following the shocks. Therefore, predicting the arrival times of these IP shocks at the near Earth space with enough lead time has become a crucial aspect in space weather forecasting. Several models aimed at forecasting the arrival time of IP shocks at 1 AU have been developed, to list a few, such as the shock time of arrival model (STOA), the interplanetary shock propagation model (ISPM) and the modified Hakamada-Akasofu-Fry/ version-2 (HAFv.2) model. These three models have been widely used in real-time prediction of the arrival time.

The STOA model is based on similarity theory of blast waves, modified by the piston-driven concept, which emanate from point explosions [1,2]. The ISPM is based on a 2.5D MHD parametric study of numerically simulated shocks that shows the organizing parameter to be the net energy input to the solar wind [3,4]. The HAFv.2 model is a "modified kinematic" solar wind model that calculates the solar wind speed, density, magnetic field, and dynamic pressure as a function of time and location [5,6]. The statistical results show that the performances of the above three models have been tested and the comparative study revealed that the performances of these three models were practically identical in forecasting the shock arrival time [6–8].

In this paper, one interplanetary shock propagation model is built up based on 1D-HD equations. The simplified 1D-HD numerical model can better reflect the most basic physical image of the disturbance's propagation in interplanetary space. A set of 68 solar events during the periods of February 1997 to October 2000 as testing data are used to evaluate the performance of the 1D-HD model. The comparisons of prediction results between our model and the models of STOA, ISPM, and HAFv.2 are also presented.

*Corresponding author (email: yzhang@spaceweather.ac.cn)

1 Model description

1.1 1D-HD equations

The time-dependent equations governing a single fluid, spherically symmetric, adiabatic solar wind are given by [9].

$$\begin{cases} \dfrac{\partial \rho}{\partial t}+v\dfrac{\partial \rho}{\partial r}+\rho\dfrac{\partial v}{\partial r}+\dfrac{2\rho v}{r}=0, \\ \dfrac{\partial v}{\partial t}+v\dfrac{\partial v}{\partial r}+\dfrac{1}{\rho}\dfrac{\partial p}{\partial r}+\dfrac{GM_S}{r^2}=0, \\ (\dfrac{\partial p}{\partial t}+v\dfrac{\partial p}{\partial r})+a^2(\rho\dfrac{\partial v}{\partial r}+\dfrac{2\rho v}{r})=0. \end{cases} \tag{1}$$

Here, as usual, ρ denotes density, v the radial speed, p the thermal pressure, a the sound speed ($a^2=\gamma p/\rho$, γ the polytropic index), G the gravitational constant, and M_S the solar mass.

In Heliosphere Equator Coordinate, V_φ and B_φ are both zero. According to the conservation of magnetic flux, radial magnetic filed satisfies $B_r=1/r^2$. Physical parameters ρ, v, B, p, t, r will be non-dimensionalized by critical point values ρ_0, v_0, B_0, p_0, τ_A, R_s. We can obtain

$$\begin{cases} \dfrac{\partial \rho}{\partial t}+\dfrac{\partial(\rho v)}{\partial r}+\dfrac{2\rho v}{r}=0, \\ \dfrac{\partial v}{\partial t}+\dfrac{\partial}{\partial r}(\dfrac{v^2}{2})+\dfrac{\beta}{2\rho}\dfrac{\partial p}{\partial r}+\dfrac{\alpha}{r^2}=0, \\ \dfrac{\partial p}{\partial t}+v\dfrac{\partial p}{\partial r}+\gamma p\dfrac{\partial v}{\partial r}+\gamma\dfrac{2pv}{r}=0, \end{cases} \tag{2}$$

where $\beta=8\pi p_0/B_0^2$ is the ratio of plasma thermal pressure to magnetic pressure, $\alpha=\dfrac{gR_\mathrm{s}}{V_\mathrm{A}}$ is the gravity acceleration dimensionless value, $\tau_\mathrm{A}=R_\mathrm{s}/V_\mathrm{A}$ and $V_\mathrm{A}=|B_0|/\sqrt{4\pi\rho_0}$ are the characteristic Alfvén time and speed, R_s is the solar radius.

1.2 Numerical grids

Due to the large scale of the computational domain from 1 R_s to 215 R_s, during which the solar wind velocity changes from subsonic to supersonic, we divide the computational domain into two domains. One domain is 1 R_s –20 R_s (called domain 1), the other is 20 R_s –216 R_s (called domain 2). For domain 1, we choose non-uniform grids $r(i)=(1+0.05)^{i-1}$; while for domain 2, we choose uniform grids $r(i)=r(i-1)+0.5$. This division completes grid system of the computational domain [1 R_s, 215 R_s]. The time increment is limited by the so-called Courant-Friedrichs-Levy condition (CFL condition) with the Courant number 0.8, $\Delta t=0.8*\Delta r/C_f$, where C_f is the maximum of the local sound speed.

1.3 Boundary conditions

In order to obtain the initial ambient solar wind conditions, the solar wind velocity, density and pressure in computational boundary should be obtained. Then we can obtain the corresponding values in the whole calculation domain by using the iteration method for difference equations.

We can choose inner boundary (on solar surface) condition and outer boundary (at 1 AU) condition. In this model, we choose outer boundary condition. For implicitly, we only use the observed background solar wind velocity at 1 AU V_sw. In order to increase the stability of the procedure, if the background solar wind velocity is less than 500 km/s, the number density at 1 AU is assumed to be 18 cm^{-3}, otherwise, it assumed to be 9 cm^{-3}. The temperature at 1 AU is assumed to be T_au. According to 1D-HD eq. (1), for steady state, T_au and V_sw satisfy the constraint relation

$$U_\mathrm{au}^2+\frac{\gamma}{\gamma-1}-H-\frac{\mu}{\gamma-1}(\frac{4}{H})^{\frac{4(\gamma-1)}{\mu}}(\frac{\gamma}{2})^{\frac{2}{\mu}}U_\mathrm{au}^{\frac{2(\gamma-1)}{\mu}}=0, \tag{3}$$

where $H=\dfrac{GM}{R_\mathrm{s}RT_\mathrm{au}}$, $U_\mathrm{au}^2=\dfrac{\rho_\mathrm{au}V_\mathrm{sw}^2}{2p_\mathrm{au}}$, $\mu=5-3\gamma$. If the solar wind velocity at 1 AU is given, the temperature at 1 AU can be determined uniquely by using Newtonian iteration method to solve eq. (3).

1.4 Initial conditions

Before solving eq. (2), Parker solar wind solution should be obtained and this will be the initial value condition. We assumed the background solar wind to be steady-state solution of eq. (2). The system does not depend on the time, thus $\partial/\partial t=0$. We substitute it into eq. (2), 1D steady-state solar wind model in dimensionless form can be obtained as

$$\begin{cases} v\dfrac{dv}{dr}+\dfrac{\beta}{2}\dfrac{1}{\rho}\dfrac{dp}{dr}+\dfrac{\alpha}{r^2}=0, \\ \rho v r^2=\mathrm{const}=C_1, \\ p\rho^{-\gamma}=\mathrm{const}=C_2. \end{cases} \tag{4}$$

According to eq. (4), we can obtain

$$v\frac{dv}{dr}(1-\frac{a^2}{v^2})=\frac{2a^2}{r}-\frac{\alpha}{r^2}, \tag{5}$$

where $a^2 = \beta\gamma p/2\rho$ is the local sound speed. From eq. (5), the critical points for $dv/dr = 0$ are located at

$$r = r_c = \frac{\alpha}{2a_c^2},$$

$$v_c^2 = a_c^2 = \frac{\beta\gamma}{2}\frac{p_c}{\rho_c},$$

where the solar wind changes from subsonic to supersonic states. Now we can write eq. (5) as

$$\frac{dv}{dr} = \frac{\frac{2a^2}{r} - \frac{\alpha}{r^2}}{v(1-\frac{a^2}{v^2})}, \tag{6}$$

where $a^2 = \frac{\beta\gamma}{2}\frac{p}{\rho} = \frac{\beta\gamma}{2}C_2C_1^{\gamma-1}(vr^2)^{1-\gamma}$. Taking the critical points into account, and using the iteration method for eq. (6), we can obtain the distribution of the background solar wind velocity depending on r in the whole calculation domain.

1.5 Simulated disturbance model

After obtaining the steady-state solar wind solution, a time-dependent pulse superimposed on the solar surface map is used to introduce the coronal explosion event such as flare and CME. Following the method of the HAF model [5,10], a high speed stream is introduced into the background solar wind stream, which propagates into the interplanetary region and causes the interplanetary shock. The temporal profile of the shock speed at the Sun is considered to be governed by a time constant (τ) that appears in the exponential expression: $V(t) = V_s(t/\tau)\exp(1-t/\tau)$, where the τ value is determined from the integrated X-ray flux in the 1–8 Angstrom GOES channel as a proxy diagnostic. It is estimated, on the usual logarithmic flux scale, by the time duration measured at one-half the distance from the pre-event background level to the peak. The shock speed rises exponentially to an assumed maximum (V_s, the Type II drift speed) and falls to a final decayed value of the background solar wind speed.

After solving the ordinary differential eq. (5), the steady-state Parker solution can be obtained. The steady background solar wind will be the initial value of eq. (2). We choose appropriate numerical scheme (here we choose Roe scheme [11]), and the partial differential equations (2) can be solved. The evolution of eq. (2) should be steady state if no disturbance is introduced. We can obtain the 1D evolution of the disturbance's propagation in interplanetary space if a disturbance is introduced on the solar surface.

1.6 Criteria for judging arrivals of IP shocks at Earth

Here, following the method used by the HAF model, a threshold of shock search index (SSI) is introduced to judge arrivals of IP shocks at Earth. In HAF model, the shock arrival time (SAT) is determined by computing predicted solar wind speed, density, and dynamic pressure at L1 spacecraft position for several days into the future [5,6]. The predicted SATs are extracted from automatic scans of the temporal profiles of the dynamic pressure simulated at L1 using a SSI: $\mathrm{SSI} = \log(\Delta P/P_{\min})$, where P is either the dynamic pressure or momentum flux; ΔP is the difference in P during consecutive 1-h time steps, and $P_{\min}$ is the minimum P value for these time steps. Shock arrival time was identified as the time of maximum SSI as long as SSI exceeds the threshold. For our present method, the threshold of SSI is assumed to be –0.4.

2 Prediction results and comparisons

For the 1D-HD model, the input parameters are the initial shock speed V_s, the duration of the solar event τ, and the background solar wind speed V_{sw}. Figure 1 shows the dependence of the transit time to 1 AU predicted by the 1D-HD model on the initial shock speed for different τ and different V_{sw}. It can be seen from Figure 1(a) that transit time decreases with the increase of the initial shock speed. And the background solar wind speed is lower; the trend of the change is more obvious. Decreasing the background solar wind speed can weaken the dependence of the transit time on the initial shock speed, particularly at the latter lower values. Figure 1(b) gives the shock transit time T versus the initial shock speed for different τ. We also found that the transit time decrease with the increase of the initial shock speed. And the transit time decreases with the shock driving time for an initial shock speed.

For testing purposes, we selected 68 solar transient events during the period from February 1997 to October 2000 [6]. In this paper, we only concern on forecasting the shock arrival time, therefore, the events without a corresponding IP shock arrival at 1 AU and those with an ambiguous relationship between the solar event and the shock at 1 AU are not included here. For the 68 events, the required input parameters are: initial shock speed (V_s), shock driving time (τ), background solar wind speed (V_{sw}) and the corresponding shock arrival time.

By applying the 1D-HD model to the data set of 68 events, we obtained the original results on the prediction of the shock arrival time. The prediction error is defined by $\Delta T_{HD} = T_{HD} - T_o$, where T_o is the observed transit times and T_{HD} is the predicted transit times by 1D-HD model.

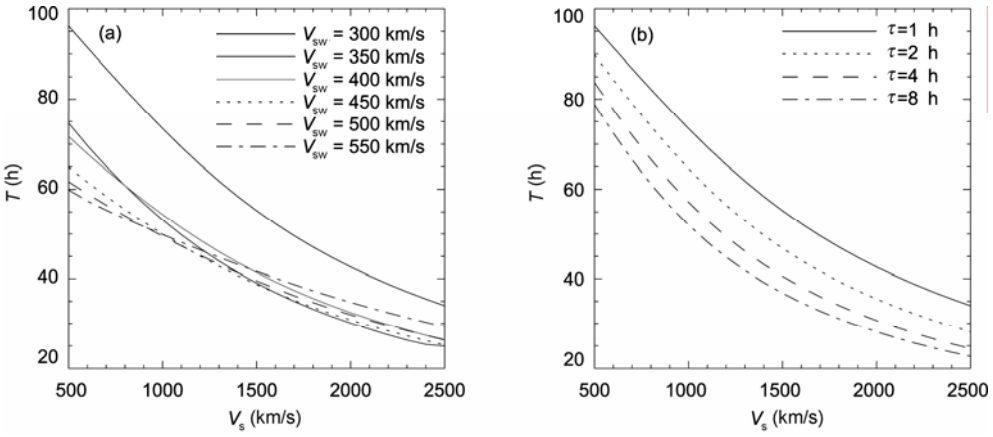

Figure 1 (a) The shock transit time T versus the initial shock speed V_s for different background solar wind speed V_{sw}. (b) The shock transit time T versus the initial shock speed for different duration time of solar event τ.

Figure 2 gives the observed transit times T_o plotted against the original predicted transit times T_{HD}. The solid line denotes the linear fitting of T_o with T_{HD}, T_o= 29.554 $+0.567\times T_{HD}$. This linear fitting does not fit the realist one (dotted line). The prediction errors of 1D-HD model are probably induced by many factors. One is that the 1-D model does not take into account the location of the transient event, which contributes to the shock arrival time. Another is that the initial shock speed would affect shock arrival time. Also, the background solar wind speed has an important effect on the shock arrival time [12,13]. The model is spherically symmetric; thus, it cannot reflect the realistic inhomogeneous solar wind. However, the background solar wind for every event cannot be given by the present models. Heinemann presented that the prediction errors would be within 9–15 h if the inhomogeneities of background solar wind was not considered [14]. Taking all of these arguments into account, we revise the results for predicting the transit times as follows: $T'_{HD} = 29.554 + 0.567\times T_{HD}$, where T'_{HD} stands for the modified transit times.

The result shows that, for the 68 events, the original mean error $\overline{|\Delta T|}$ of the 1D-HD model is 13.43 h, while the mean error is 12.75 h after our modification of the first prediction results. The prediction result is improved after this modification. Table 1 gives the mean absolute errors of STOA, ISPM, HAFv.2, and 1D-HD models. The mean errors of STOA, ISPM, and HAFv.2 models are 14.09 h, 13.87 h, and 14.10 h, respectively. The mean absolute errors of these models are nearly identical, which shows similar capability of forecasting the IP shock arrival time among these models.

Figure 3 gives the histogram of error in the predicted transit time for the 1D-HD model. The histogram shows a Gaussian distribution with a peak around zero after modified the prediction results. This property of approximate normal distribution demonstrates that the propagation of the interplanetary disturbances are mainly accounted for the model and may be influenced additionally by other factors. However, other error sources, such as coronal density distribution, complex heliospheric environments, and solar wind inhomogeneities [15–17], can also influence the propagation and arrival of IP shocks and may lead to complicated distributions of the predicted transit time. And these error sources can explain, at least partly, the fact that the mean absolute errors of the model are all above 12 h.

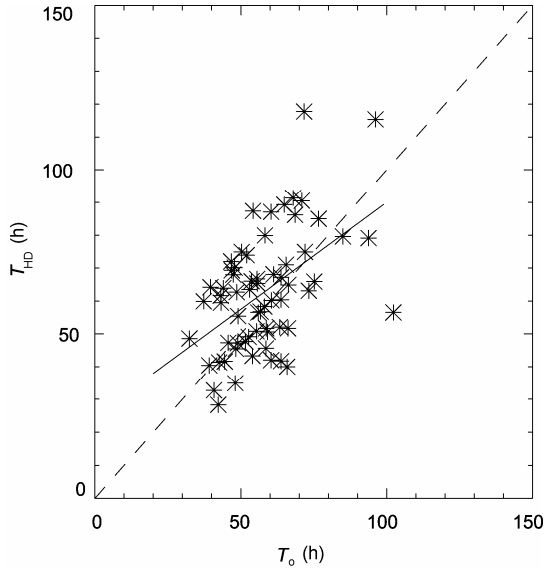

Figure 2 The observed transit time T_o plotted versus the predicted transit time T_{HD}. The solid line denotes a linear fitting.

Table 1 Averaged absolute errors of STOA, ISPM, HAFv.2, and 1D-HD models

Models	Averaged absolute errors (h)
STOA	14.09
ISPM	13.87
HAFv.2	14.10
1D-HD（original）	13.43
1D-HD（modified）	12.75

As for the relative error of predictions, i.e.,

$$\sigma = \frac{\left|T_{\rm o} - T_{\rm pred}\right|}{T_{\rm o}}.$$

The prediction test for σ shows that, for selected 68 events, 29% of all the events have the relative error less than 10%, 66% have relative error less than 30%, and 90% have the relative error less than 50% before modification of the prediction results. But after modification, 31% of all the events have the relative error less than 10%, 75% have the relative error less than 30%, and 84% have the relative error less than 50%. It is found that the prediction result is improved for the relative error less than 10% after modification. For the STOA model, 24%, 63%, and 78% of all the event have the relative error less than 10%, 30%, and 50%, respectively. For the ISPM model, 21%, 50%, and 59% of all the events have the relative error less than 10%, 30%, and 50%, respectively. For the HAFv.2 model, 31%, 72%, and 93% of all the events have the relative error less than 10%, 30%, and 50%, respectively. We can see from Table 2 that the performances of the four models in terms of relative errors are nearly identical as well.

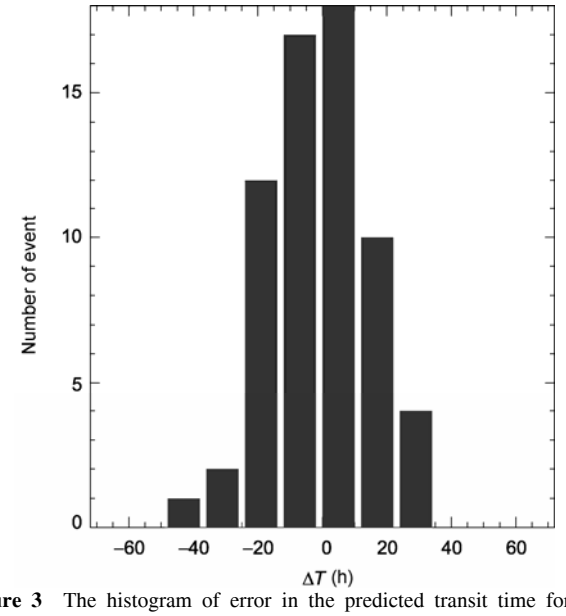

Figure 3 The histogram of error in the predicted transit time for the 1D-HD model.

Table 2 Comparison of prediction results from STOA, ISPM, HAFv.2 and 1D-HD models

Models	Event percentage		
	$\sigma \leqslant 10\%$	$\sigma \leqslant 30\%$	$\sigma \leqslant 50\%$
TOA	24%	63%	78%
ISPM	21%	50%	59%
HAFv.2	31%	72%	93%
1D-HD (original)	29%	66%	90%
1D-HD (modified)	31%	75%	84%

3 Conclusions and discussion

In this paper, one interplanetary shock propagation model is built up based on 1D-HD equations by using Roe scheme. Gonzalez et al. [18] used a one-dimensional, hydrodynamic single-fluid model to simulate eight CMEs at two kinds of ambient solar wind conditions and obtained some statistical results. These results show that for these cases the travel time depends not only on the CME initial speed, but on the ambient wind and other CME characteristics. However, the simulations show that the arrival time of very fast CMEs ($V_{\rm cme}$ >1000 km/s) has a smaller dispersion and therefore predictions can be made with reasonable accuracy [18]. Our model also obtains the same results: the arrival time would be affected by initial shock speed and the background shock speed. The transit time decreases with the increase of the initial shock speed. And the background solar wind speed is lower; the trend of the change is more obvious. Decreasing the background solar wind speed can weaken the dependence of the transit time on the initial shock speed, particularly at the latter lower values.

We used 68 solar events during the period of February 1997 to October 2000 as test events for 1D-HD model to predict the shock arrival time. The input parameters for this model are initial shock speed, shock driving time and background solar wind speed. The prediction test for selected 68 events tell us that 31% of all the events have the relative error less than 10%, 75% have the relative error less than 30%, and 84% have the relative error less than 50%. This shows that our model could be practically equivalent to the STOA, ISPM, HAFv.2 models in forecasting the shock arrival time.

However, like other similar arrival time prediction models, this present 1D-HD model is just a simple as well as ideal one with its own shortcomings. Firstly, coronal mass ejection is a complicated space plasma process, and we only use three kinds of observing data to simulate the disturbance coarsely, neglecting the location of the CME. The prediction result is not precise enough as being imagined. Secondly, we do not consider the forecasting model for a specific event, but only present a method to predict the shock's arrival time by inputting the observing data. So there would be some prediction errors for a large number of events, which are only on a statistic sense. For the simulation of successive events, there would be interactions among multi waves in interplanetary space [12,13]. For these events, the former event's disturbance can be seen as the background condition of the latter event. Thirdly, this model is a 1-D model, which can only partly reflect the physical picture of the disturbance's propagation. The simplified 1-D redial magnetic field makes the evolution equations degenerate into HD equations. However, the occurrence of actual processes is controlled by MHD equations. If 2-D or 3-D simulation and the changes of the normal magnetic field are considered, the reliability of this model would be improved. All

these deserve future consideration.

This work was supported by the National Natural Science Foundation of China (*Grant Nos. 40890162, 40874078, 40536029 and 40523006*), *National Basic Research Program of China* (*Grant No. 2006CB806304*), *Specialized Research Fund for State Key Laboratories and Special Fund for Public Welfare Industry* (*Meteorology*) (*Contract GYHY200806024*).

1 Dryer M, Smart D F. Dynamical models of coronal transients and interplanetary disturbances. Adv Space Res, 1984, 4: 291−301
2 Smart D F, Shea M A. A simplified model for timing the arrival of solar-flare-initiated shocks. J Geophys Res, 1985, 90: 183−190
3 Smith Z, Dryer M. MHD study of temporal and spatial evolution of simulated interplanetary shocks in the ecliptic plane within 1 AU. Solar Phys, 1990, 129: 387−405
4 Smith Z K, Dryer M. The Interplanetary Shock Propagation Model: A model for predicting solar-flare-caused geomagnetic sudden impulses based on the 2-1/2D MHD numerical simulation results from the Interplanetary Global Model (2DIGM), NOAA Technical Memorandum, ERL/SEL-89. 1995
5 Fry C D, Sun W, Deehr C S, et al. Improvements to the HAF solar wind model for space weather predictions. J Geophys Res, 2001, 106: 20985−21002
6 Fry C D, Dryer M, Smith Z, et al. Forecasting solar wind structures and shock arrival times using an ensemble of models. J Geophys Res, 2003, 108, doi:10.1029/2002JA009474
7 Smith Z K, Dryer M, Ort E, et al. Performance of Interplanetary shock prediction models: STOA and ISPM. J Atmos Sol-Terr Phys, 2000, 62: 1265−1274
8 McKenna-Lawlor S, Dryer M, Kartalev M D, et al. Near real-time predictions of the arrival at the Earth of flare-generated shocks during Solar Cycle 23. J Geophys Res, 2006, 111, A11103, doi:10.1029/2005JA011162
9 Nayagawa Y, Steinolfson R S. Dynamical response of the solar corona. Astrophys J, 1976, 207: 296−299
10 Hakamada K, Akasofu S I. Simulation of three-dimensional solar wind disturbance and resulting geomagnetic storms. Space Sci Rev, 1982, 31: 3−70
11 Cargo P, Gallice G. Roe matrices for ideal MHD and systematic construction of Roe matrices for systems of conservation laws. J Comput Phys, 1997, 136: 446−466
12 Wu C C, Feng X S, Wu S T, et al. Effects of the interaction and evolution of interplanetary shocks on “background” solar wind speeds. J Geophys Res, 2006, 111, A12104, doi:10.1029/2006JA011615
13 Xiong M, Zheng H N, Wang Y M, et al. A numerical simulation on the solar-terrestrial transit time of successive CMEs during November 4−5, 1998 (in Chinese). Chin J Geophys, 2005, 48: 731−738
14 Heinemann M. Effects of solar wind inhomogeneities on transit times of interplanetary shock waves. J Atmos Sol-Terr Phys, 2002, 64: 315−325
15 Moon Y J, Dryer M, Smith Z, et al. A revised shock time of arrival (STOA) model for interplanetary shock propagation: STOA-2. Geophys Res Lett, 2002, 29, 1390, doi:10.1029/2002GL014865
16 Cho K S, Moon Y J, Dryer M, et al. A statistical comparison of interplanetary shock and CME propagation models. J Geophys Res, 2003, 108: 1445−1452
17 Feng X S, Zhao X H. A new prediction method for the arrival time of interplanetary shocks. Sol Phys, 2006, 238: 167−186
18 Gonzalez-Esparza J A, Lara A, Perez-Tijerina E, et al. A numerical study on the acceleration and transit time of coronal mass ejections in the interplanetary medium. J Geophys Res, 2003, 108, 1039, doi: 10.1029/2001JA009186